Research

# Systematic determination of patterns of gene expression during *Drosophila* embryogenesis

Pavel Tomancak*, Amy Beaton*, Richard Weiszmann†, Elaine Kwan*, ShengQiang Shu†, Suzanna E Lewis†, Stephen Richards†‡, Michael Ashburner§, Volker Hartenstein¶, Susan E Celniker†‡ and Gerald M Rubin*†

Addresses: *Howard Hughes Medical Institute, Department of Molecular and Cell Biology, University of California at Berkeley, 539 Life Sciences Addition, Berkeley, CA 94720-3200, USA. †Berkeley Drosophila Genome Project, ‡Genome Sciences Department, Lawrence Berkeley National Laboratory, Berkeley, CA 94720, USA. §Department of Genetics, University of Cambridge, Cambridge CB2 3EH, UK. ¶Department of Molecular Cell and Developmental Biology, University of California Los Angeles, Los Angeles, CA 90095, USA.

Correspondence: E-mail: gerry@fruitfly.org

Published: 23 December 2002

*Genome* ***Biology*** 2002, **3(12)**:research0088.1–0088.14

The electronic version of this article is the complete one and can be found online at http://genomebiology.com/2002/3/12/research/0088

© 2002 Tomancak *et al.*, licensee BioMed Central Ltd
(Print ISSN 1465-6906; Online ISSN 1465-6914)

Received: 3 October 2002
Revised: 18 November 2002
Accepted: 19 November 2002

## Abstract

**Background:** Cell-fate specification and tissue differentiation during development are largely achieved by the regulation of gene transcription.

**Results:** As a first step to creating a comprehensive atlas of gene-expression patterns during *Drosophila* embryogenesis, we examined 2,179 genes by *in situ* hybridization to fixed *Drosophila* embryos. Of the genes assayed, 63.7% displayed dynamic expression patterns that were documented with 25,690 digital photomicrographs of individual embryos. The photomicrographs were annotated using controlled vocabularies for anatomical structures that are organized into a developmental hierarchy. We also generated a detailed time course of gene expression during embryogenesis using microarrays to provide an independent corroboration of the *in situ* hybridization results. All image, annotation and microarray data are stored in publicly available database. We found that the RNA transcripts of about 1% of genes show clear subcellular localization. Nearly all the annotated expression patterns are distinct. We present an approach for organizing the data by hierarchical clustering of annotation terms that allows us to group tissues that express similar sets of genes as well as genes displaying similar expression patterns.

**Conclusions:** Analyzing gene-expression patterns by *in situ* hybridization to whole-mount embryos provides an extremely rich dataset that can be used to identify genes involved in developmental processes that have been missed by traditional genetic analysis. Systematic analysis of rigorously annotated patterns of gene expression will complement and extend the types of analyses carried out using expression microarrays.

## Background

Cell-fate changes that occur during development are almost always accompanied by changes in gene expression. Thus detailed knowledge of the spatial and temporal expression patterns for all genes will be an important step in deciphering the complex regulatory networks governing development.

Two methods have been used successfully to determine gene-expression patterns on a large scale - RNA *in situ* hybridization [1] and DNA microarrays [2-4]. Whole-mount RNA *in situ* hybridization is a well-established approach for determining precise spatial gene-expression patterns [5,6], and can be done in high-throughput fashion [7,8]. Although RNA *in situ* hybridization is carried out on fixed tissues, examining a large number of differently staged specimens provides an overview of the dynamic changes in gene-expression patterns that occur during development. Expression patterns can be documented by microscopy coupled to digital photography and distributed on the web as a valuable resource to the research community.

Approaches using DNA microarrays have been successful in studying genome-wide transcriptional regulation during animal development [9-11], but suffer from several limitations. In multicellular organisms, cell division and differentiation leads to an increase in tissue complexity throughout development, but whole-animal microarray analysis cannot document this spatial information. One can attempt to isolate mRNA from every tissue at different developmental stages, measure gene expression, and assign expression indexes to every tissue at every time for every gene, in order to recreate the entire developmental expression pattern. This is a formidable task. Moreover, the quantitative comparison of expression levels for a given gene, or among different genes, in multiple experiments is complicated by differential hybridization kinetics and cross-hybridization properties of each target-probe pair [12,13]. On the other hand, microarray profiles do provide a quantitative overview of the relative changes in each gene's expression level across time.

We used high-throughput RNA *in situ* hybridization to assemble a database of gene-expression patterns during embryonic development of *Drosophila melanogaster*. cDNA clones are available for 70% of all *Drosophila* genes [14-16], providing a convenient source of templates for generating specific hybridization probes for the majority of genes. *Drosophila* embryogenesis has been studied extensively, providing a strong foundation of knowledge for our project [17]. Moreover, studies of a large number of individual genes have documented the diversity of gene-expression patterns that occur during *Drosophila* embryogenesis and established the importance of tissue-specific gene expression for development.

Here we describe the molecular, microscopic, and computational methods we used to produce a database of *Drosophila* embryonic expression patterns that integrates results obtained by *in situ* hybridization to whole-mount embryos and by expression microarrays. Expression patterns are documented by assembling digital photographs of individual staged embryos that are ordered to visualize time-dependent changes. To facilitate computational analysis, these patterns are annotated using a controlled vocabulary that captures developmental and spatial relationships between embryonic tissues. We used hierarchical clustering of the annotation terms to group together genes with similar expression patterns as well as tissues with similar sets of expressed genes. We report several noteworthy observations based on our initial data, which provide a glimpse of the diversity of gene expression and the utility that will derive from a complete atlas of gene-expression patterns during *Drosophila* development. All production, image and annotation data are stored in a relational database and presented in searchable form on the web [18].

## Results and discussion

### Overview of the high-throughput *in situ* hybridization procedure

The starting material for the production of hybridization probes was the set of cDNA clones that comprise the *Drosophila* Gene Collection [14-16]. The cDNAs were amplified in 96-well PCR plates using a vector-specific primer set that introduces a promoter for the production of a digoxigenin-labeled antisense RNA probe by *in vitro* transcription. PCR products were sized to confirm the identity of each clone and that the PCR reaction was successful (Figure 1a). The strength of each probe was determined by a dot-blot color reaction (Figure 1b). These data were entered into a relational database and later used as experimental controls when assessing the outcome of each hybridization experiment.

RNA probes were hybridized to fixed *Drosophila* embryos [19] in 96-well plates (see Materials and methods). Three genes (*engrailed, hunchback, brinker)* with well-described expression patterns were included in each 96-well plate and used to monitor hybridization efficiency. After hybridization, each plate was examined to determine the morphology of the embryos, quality of the staining and proportion of wells that showed staining (Figure 1c). A plate containing embryos of acceptable morphology, relatively free of staining artifacts and with more than 50% of the wells stained was considered successful and passed on to the image-acquisition stage.

Embryos from successful plates were mounted onto microscope slides. Low-magnification digital images of a group of embryos were taken (Figure 1d) to provide a permanent record of the hybridization in each well. Low-resolution imaging was insufficient to document highly restricted expression patterns or to identify small subsets of cells. For that purpose, each slide was examined under higher magnification using a Zeiss Axiophot optical microscope. At this stage, a human annotator carefully examined the entire slide, taking a large number of high-resolution digital photographs that document that gene's expression pattern (Figure 1e). All images were submitted to the relational database using a web-based annotation tool. We determined the success of each hybridization experiment by taking into account the results of the agarose gel analysis of PCR products, dot-blot

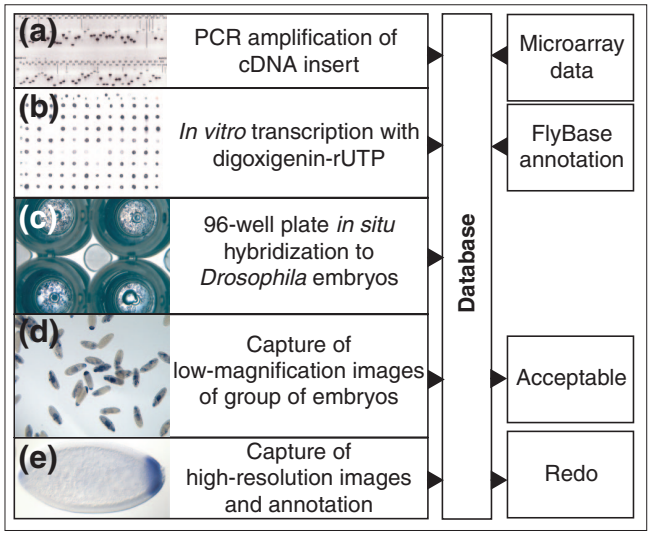


**Figure 1**
Overview of the *in situ* production pipeline. **(a-e)** Examples illustrating each step of the high-throughput production of RNA *in situ* patterns. (a) Photograph of an agarose gel showing PCR products from a single 96-well plate. The vertical lines mark failed PCR reactions. (b) Nylon membrane spotted with 96 RNA *in situ* probes and stained to reveal the incorporation of digoxigenin. Missing or weak spots indicate a failed probe reaction. (c) Four wells of a 96-well plate, each containing about 200 embryos. (d) Low-resolution photograph of stained embryos. (e) High-resolution photograph of an individual embryo. All image and textual data are entered into a MySQL relational database and integrated with microarray data and previously published expression patterns.

analysis of probes, microarray data (described below), available information from public databases, and the quality of the captured images. Each experiment had two possible outcomes: either the observed expression pattern or the absence thereof was consistent with the available data, or there was a discrepancy indicating failure at some point and that the experiment needs to be repeated. About 13% of the *in situ* experiments failed, as a result of either the absence of a PCR product (9.2%) or a poor probe-labeling reaction (3.4%), which resulted in no detectable staining. Additionally, probes that generated expression patterns inconsistent with previously published data (0.3%) or the microarray expression profile (7%) were rejected as being possibly mislabeled or cross-contaminated. Overall, we obtained useful expression data for 2,179 out of 2,721 (80%) of the genes whose transcript distribution we analyzed.

### Documenting expression patterns by digital photography

We captured high-resolution photographs of the 1,388 genes (63.7% of the 2,179 successfully asssayed genes) that exhibited some level of tissue-specific gene expression. The captured images were ordered according to the developmental stage of the embryos in order to visualize the change of the expression pattern over time. Embryogenesis is traditionally divided into a series of consecutive stages distinguished by morphological markers [20]. The duration of developmental stages range from 15 minutes to more than 2 hours; therefore the stages of development were differentially represented in our embryo collections (see Materials and methods). Some consecutive stages, although morphologically distinguishable, differ very little in terms of changes in gene expression, whereas other stage transitions, such as the onset of zygotic transcription or organogenesis, are accompanied by massive changes in gene expression. We divided the first 16 stages of embryogenesis into six convenient stage ranges (stages 1-3, 4-6, 7-8, 9-10, 11-12 and 13-16). Each captured image is assigned to a stage range, and for each stage range a number of images are taken so that all stages within the range are represented. The groups of images assigned to a stage range are arranged in the web-based annotation tool from left to right so that one can follow the pattern through development (Figure 2).

We took, on average, 16 individual images for each gene; however, the number of images per gene varies from 1 to 80. This variability reflects our strategy to document highly dynamic, complex, novel and otherwise notable patterns extensively, while progressively lowering the number of images documenting common or simple expression patterns. The number and type of images collected for each probe were chosen so as to allow an embryologist to reconstruct the expression pattern as if they were examining the stained embryos under a microscope.

Although the *in situ* hybridization analysis is performed on fixed tissues, the ability to take many snapshots of developmental processes and to order them allows us to reconstruct dynamic developmental events. For example, we can visualize the progressive segmental proliferation of the fat body (Figure 3a-e) or follow the dispersal of blood-cell precursors throughout the embryo (Figure 3f-j).

Many genes are either not expressed at all during embryogenesis or their expression is not tissue specific. Several canonical examples of these staining patterns were captured, and then only textual annotation and a low-magnification image were used to document additional occurrences. A total of 791 genes (36.3% of the 2,179 genes successfully assayed) were not documented by high-resolution images. These were assigned to one of the following four classes: 362 (16.6%) do not appear to be expressed during embryogenesis; 21 (1%) are not maternally contributed but are ubiquitously expressed in the developing embryo; 317 (14.5%) are exclusively maternally expressed; and 91 (4.2%) show both maternal and ubiquitous zygotic expression.

### Microarray data as independent measurements of RNA expression patterns

We used microarray time-course expression profiles as independent measurements to ascertain the accuracy of the captured expression patterns. For the microarray measurements

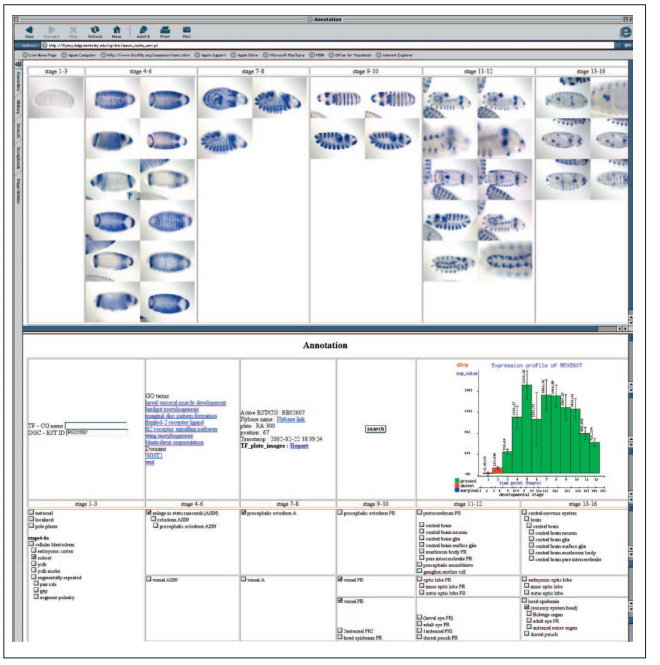


**Figure 2**
Imaging expression patterns during embryogenesis. Screen shot of the web-based tool used to organize and annotate captured images. The figure shows the categorization of images in six stage ranges, reflecting developmental time, presented left to right. The annotation terms are similarly arranged from left to right and grouped from top to bottom according to related organ systems. Groups of images at a given stage range will be associated with groups of annotation terms appropriate for that stage range. Microarray profiles and links to public databases are also included.

to be truly independent, it was important that no single clone contamination or misidentification event be able to affect the integrity of both the microarray and *in situ* hybridization result. Existing microarray datasets, such as that reported in [21], were generated using spotted cDNA arrays [13] derived from the same DGC clone set [14-16] that we used for the *in situ* probes, and were therefore unsuitable as independent controls. For this reason, we chose to generate a new dataset using Affymetrix GeneChip technology [3], where the oligonucleotide probes are designed directly from the genome sequence and do not depend on the cDNA clone identity. For the microarray analysis, we divided embryogenesis into 12 1-hour time windows, collected three independent embryo samples for each time window, and hybridized total RNA from each sample to the GeneChip *Drosophila* Genome Array. As each embryo sample contained a distribution of different ages, we examined the distribution of morphological stage-specific markers in each sample to correlate the time-course windows with the nonlinear scale of embryonic stages. As described above, the image data are organized into groups of images associated with a range of embryonic stages. Both the image and the microrray datasets are thus linked by a common time scale of developmental stages. This facilitates the direct comparison of the *in situ* staining patterns with microarray expression indexes. Figure 4 shows the comparison of array and image data for a highly unusual gene-expression pattern. In the absence of any additional information on the cDNA clone LD43816 (*CG4702*), the contrast between the heavy staining seen in late embryos and the earlier highly restricted pattern might suggest the possibility of probe contamination. However, when stage-specific images are compared with the microarray profile, the expression profile is consistent with the *in situ* hybridization data. Although high-throughput *in situ* hybridization is subject to potential sources of error, such as cross-contamination during PCR amplification or probe synthesis, using microarray expression data in parallel helped us avoid erroneous pattern assignment.

For a number of reasons, correlating staining patterns and microarray values is not straightforward. First, the intensity of *in situ* hybridization staining is dependent on the strength of the probe and length of the color reaction. Second, it is not possible to distinguish weak ubiquitous staining from strong staining in a small subset of cells using whole-embryo microarray data. For microarray data, it is broadly accepted that relative comparison of independent measurements for

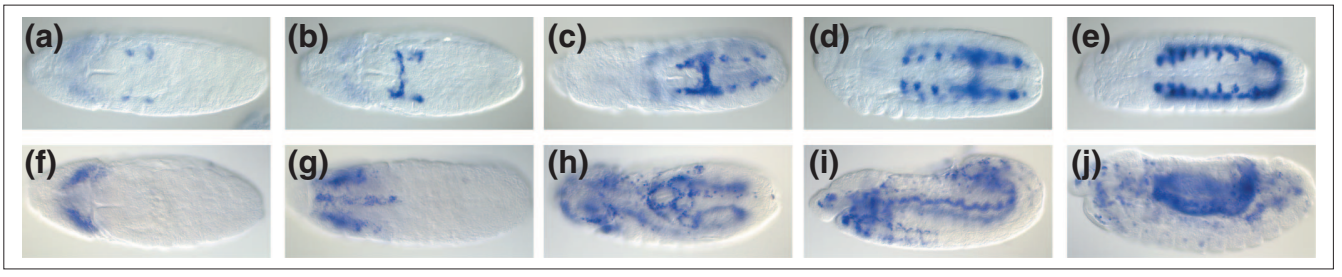


**Figure 3**
Visualization of dynamic developmental processes. **(a-e)** Series of five embryos stained with a probe (*bgm*) highlighting the fat-body primordium and revealing dynamic aspects of segmental fat-body specification. Ventral view with anterior to the left. **(f-j)** Series of five embryos stained with a probe (*CG4829*) visualizing the lamellocyte precursors. The staining reveals the spreading pattern of lamellocytes across the embryo and the 'hitchhiking' of migrating cells on the retracting germ band.

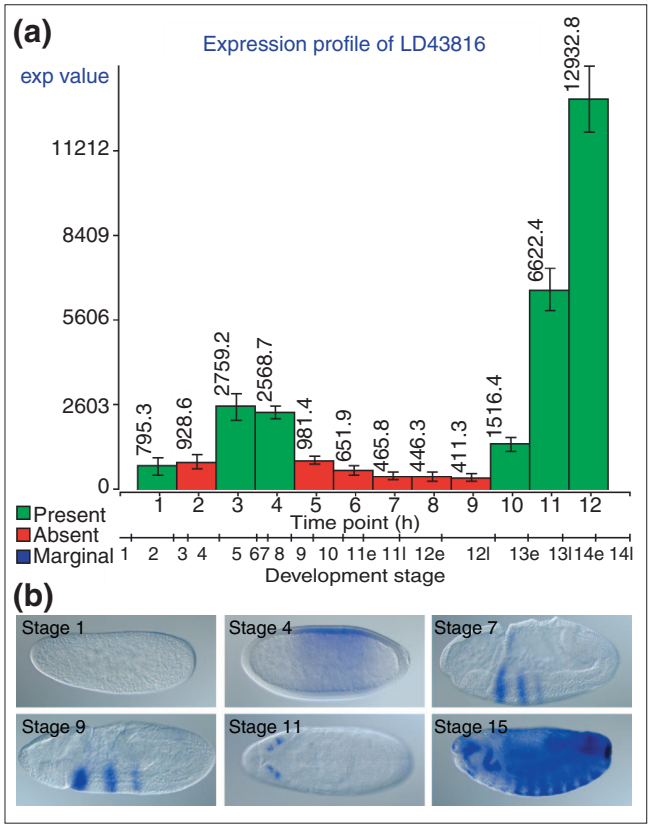


**Figure 4**
Comparison of image and microarray data for gene *CG4702*. **(a)** A microarray expression profile of the gene *CG4702*, represented by EST clone LD43816. Consecutive time points representing RNA samples from differentially aged 1-h embryo collections are presented on the *x*-axis, while the *y*-axis represents the scale of absolute expression indexes as analyzed by dChip analysis software [37]. Error bars represent standard error of the measurements, which were carried out independently on three separate embryo collections; the number next to each bar is the mean of the three measurements. The color of the bar reflects the categorization of each measurement on the basis of a statistical analysis performed by the Affymetrix Microarray Suite software package. Green represents present; red, absent. Because of the sensitivity limitations of the GeneChip measurements and the conservative nature of the software, absent calls do not necessarily imply lack of gene expression. The secondary *x*-axis correlates the microarray sample time points with stages of embryogenesis. **(b)** Images of six staged embryos illustrating expression during development of the same gene characterized above by microarray analysis. Each image comes from a different stage range (stages 1-3, 4-6, 7-8, 9-10, 11-12, and 14-16). Lateral view, anterior to the left.

the same gene are reliable, whereas absolute intensities across different genes are not, especially for low expression values [12]. For all these reasons, the most useful factor in correlating microarray and image data is the relative fluctuation of signal intensity over the course of development. Figure 5 shows 14 examples of distinct expression profiles that exhibit strong correlations between microarray and image data. The expression patterns of all these genes (except CG8782) have been previously described, providing independent confirmation that each profile is correct. Clear-cut correlations between microarray and *in situ* hybridization data as seen in Figure 5 are possible when the expression pattern exhibits changes over time. For monotonically expressed genes, the correlation is rather subjective and relies on absolute intensities of both microrarray and *in situ* hybridization signals. In 7% of the experiments, we rejected the observed expression pattern because of an obvious mismatch with the microarray expression profile; such cases account for approximately one third of the genes whose analysis will need to be repeated.

Large-scale production of RNA *in situ* data is prone occasionally to produce false-negative results due to failures in probe production and hybridization. Microarray data are useful to identify experiments where the RNA *in situ* hybridization failed but the given gene is highly expressed. High absolute microarray-derived gene-expression values, coupled with either a continuous profile across the time course or distinct on/off periods during the time course, is a reliable indication that a gene is expressed. Low expression values, and a lack of consistency among replicate experiments, may indicate that a gene is not transcribed during embryogenesis. However, if a given gene is active in only a very small subset of cells, the microarray results from a whole-animal experiment may not be sensitive enough to detect its expression. Therefore, even with the microarray data at hand, it is not possible to avoid completely false negatives for low-abundance transcripts.

## Textual annotation of gene-expression patterns and assembly of a public database

To provide searching capability beyond queries for a specific gene, we rigorously annotated the gene-expression profiles using a controlled vocabulary. We used human annotation, rather than automated approaches based on pattern-recognition algorithms, because of the overwhelming complexity of annotation. Variation in morphology and incomplete knowledge of the shape and position of various embryonic structures make computational approaches impracticable at present. Moreover, a human annotator does not only take into account the image data, but also integrates other information such as the microarray profile and previously published data into the final assessment of the expression pattern. In our project, a single person carried out the initial annotation, resulting in a highly consistent dataset.

Annotation of gene-expression patterns that change dynamically over time poses a significant challenge. There is a need to have a specific name not only for the final developed embryonic structures but also for all the developmental intermediates that precede them. Every terminally differentiated structure of the embryo descends from a group of cells within the cellular blastoderm epithelium [17]. We used this embryological concept to define a set of embryonic structure names that depict a 'path' describing the development of each organ. Four basic categories of developmental structures, called

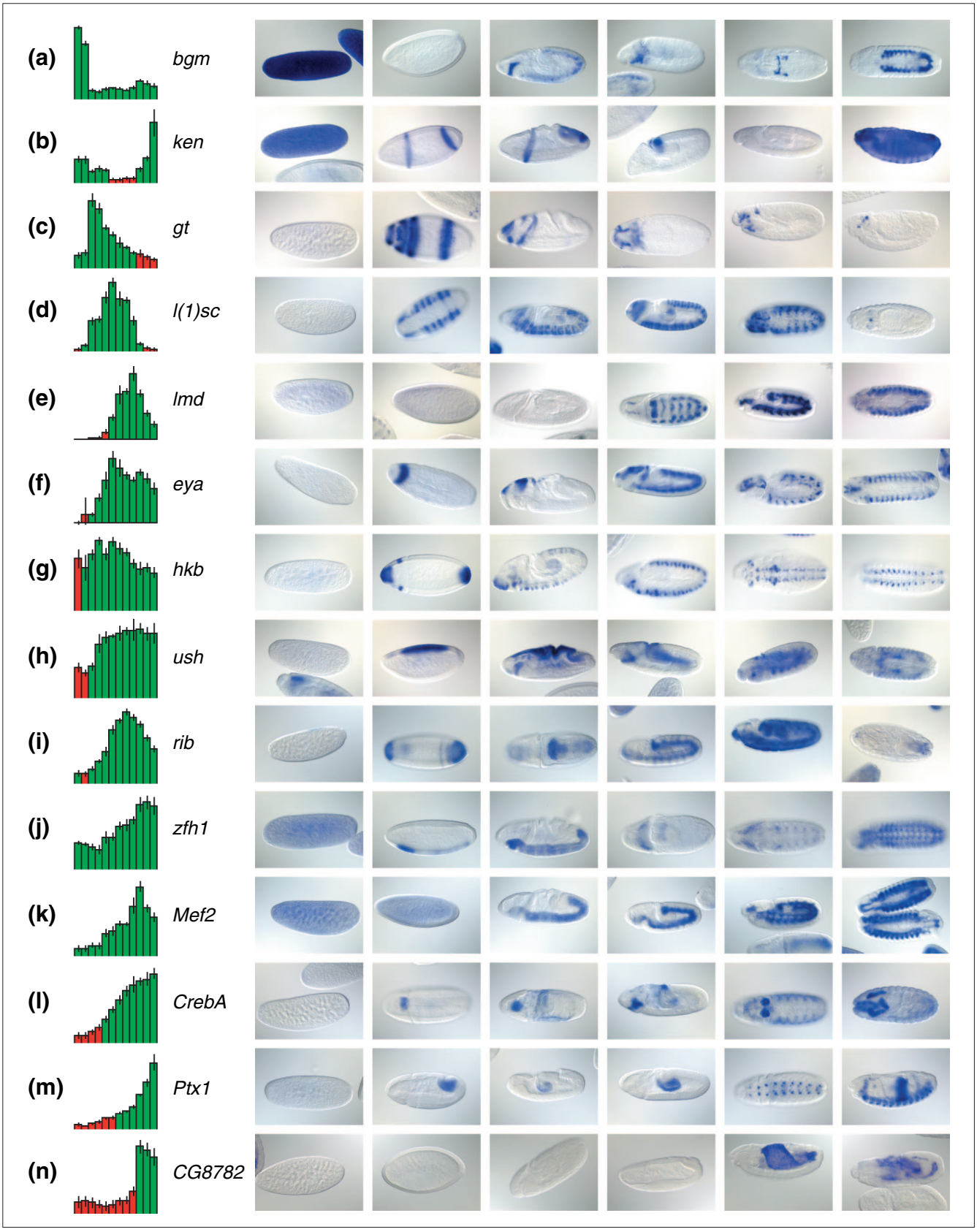


**Figure 5** *(see the legend on the next page)*

anlage in statu nascendi, anlage, primordium and organ, are distinguished.

At the end of embryogenesis, organs can be distinguished by their unique morphology and function (for examples, see Figure 6a). Traditionally, two types of developmental intermediates that precede the terminally differentiated organ have been defined: anlage and primordium (for examples, see Figure 6a). An anlage is defined as a morphologically indistinct group of contiguous cells, established by lineage tracing, that gives rise to an individual organ. Anlagen for most organs can be distinguished at the late cellular blastoderm or gastrula stage (stages 5-9). A primordium can be recognized on the basis of its distinct morphology. A primordium will give rise to one or more differentiated organs. We have included the germ layers in the primordium category. Primordia develop from anlagen but an anlage - for example, a group of cells defined by gene expression that will give rise to a subset of an organ - can also be part of a primordium. Individual names are connected by relationships that define the way the respective tissues develop from one another or encompass one another.

Many genes whose expression is ultimately restricted to, and required for the determination of, a specific anlage initially appear in a larger area. This dynamic expression may reflect the working of an underlying molecular network of activating and inhibitory factors which only gradually succeed in directing expression of a given gene to a specific subset of cells which thereby become defined as a distinct anlage. We propose the term 'anlage in statu nascendi' (*in statu nascendi* can be loosely translated as 'in the process of being formed') for the larger domain from which a specific anlage originates. Anlagen in statu nascendi can only be visualized by gene-expression analysis. They typically appear at the cellular blastoderm stage and resolve into specific anlagen towards the beginning of gastrulation (examples are given in Figure 6a).

Using this naming scheme we are able to describe the development of embryonic structures starting from anlage in statu nascendi at the cellular blastoderm stage through a series of developmental intermediates - anlage and primordia - to a differentiated embryonic structure. For example, the transcription factor single minded is expressed in the glial cells of the mature embryo [22]. The origin of this expression pattern can be traced from the mesectoderm anlage in statu nascendi, to the mesectoderm anlage, to the mesectoderm (or midline primordium ) and, finally, to the mature midline glial cells (Figure 6b).

In the annotation tool (Figure 2), only those annotation terms that describe structures present within a specific stage range are displayed beneath the images of embryos from that stage. Annotation terms are organized into a hierarchy according to the developmental relationship between them. Using the annotation tool, one can follow and describe the development of each structure through its intermediates by observing the development of the staining pattern and selecting the appropriate annotation terms. Integration of image data with the predefined developmental hierarchy is one of the prime goals of our annotation effort.

One advantage of storing the data in a database is the ability to query the data and compare results in a rigorous manner. However, this is only possible if the data that are entered into the database are themselves rigorously controlled. Comparisons of biological data are complicated by the lack of standards in both reagents and nomenclature. We provide a standardized set of *in situ* expression images prepared using the same hybridization probes, laboratory protocols, and descriptive nomenclature. For the nomenclature we needed an agreed vocabulary of terms to describe the different anatomical features of the *Drosophila* embryo and the different stages of embryonic development. This was provided to us by the controlled vocabularies of anatomy and development that have been constructed by FlyBase [23] over the past few years. A further advantage in using these vocabularies is that our data will be recorded in a way that is wholly consistent with that used by the FlyBase curators, who record gene-expression data from the scientific literature.

The FlyBase controlled vocabularies are organized as a directed acyclic graph (DAG). In a DAG the terms are the

**Figure 5** *(see the figure on the previous page)*
Correlation of image and microarray data. **(a-n)** Fourteen examples of correlations between microarray and image data for genes with known expression patterns. Microarray expression profiles are shown on the left. Red is absent, green is present, and vertical lines on bars represent error bars of triplicate measurements. On the right are six representative images, one for each stage range specified in Figure 4, ordered according to developmental time to allow visual correlation with the corresponding array profile. Anterior to the left. The most straightforward comparisons occur when gene expression comes on (e,n) or is turned off abruptly (a,b), corresponding to the absence or presence of *in situ* staining respectively. In many cases, the absent/present call misses the expression of genes confined to a small subset of tissues (c,m). (l) Gene-expression levels increase, followed by an increase in staining intensity that occupies approximately the same proportion of the embryo. (f) The increase in microarray intensity reflects an increase in the number of cells in the embryo showing gene expression across time. (c) Fading expression is indicative of the restriction of gene expression to a smaller subset of cells as development proceeds. Frequently, a microarray profile will show both types of fluctuations, and in that case the visual correlation is rather subjective (g,h), unless accompanied by a clear-cut qualitative change (d,e,i). (k) Genes transcribed both maternally and zygotically have no 'off' period during our developmental time course. (j) The decrease in abundance of maternal transcript often overlaps with emergence of zygotic transcript, leading to the flattening of the early portion of the microarray profile.

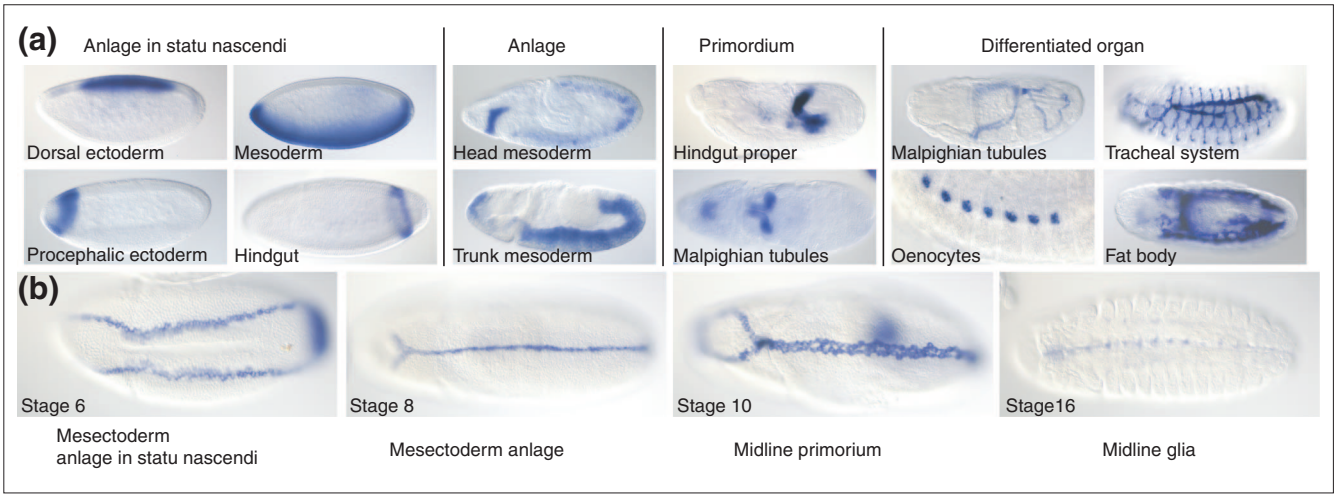


**Figure 6**
Textual annotations using controlled vocabularies. **(a)** General categories of anatomical terms and the developmental relationships between them. We distinguish four types of anatomical structures: 'anlage in statu nascendi', 'anlage', 'primordium' and differentiated 'organs'. Below each heading are examples of staining patterns that illustrate a specific instance of that category of developmental structure. The examples are not developmentally related. Anlage in statu nascendi, anlage and primordium become suffixes to the specific name of a structure, such as dorsal ectoderm anlage in statu nascendi, head mesoderm anlage and Malpighian tubule primordium. Differentiated organs are named without a suffix, for example fat body. **(b)** Embryos at the indicated stages stained with a probe for the gene *single minded* reveal the developmental origin of the midline glia. Ventral view, anterior to the left.

nodes in the graph and the relationships between terms are the arcs of the graph. A DAG has two characteristics that make it extremely useful for describing vocabularies. First, the graph is directed, which means that the reciprocal roles of two terms in a relationship are unequal. Thus, the 'parent' term may be a less specific and the 'child' term more detailed. Second, unlike strict hierarchies, a child term may have more than one parent terms. This data structure is the same as that used by the Gene Ontology (GO) Consortium for terms that are used to annotate gene products [24].

The FlyBase controlled vocabulary uses three classes of relationship between parent and child terms. The first of this is 'is an instance of'; for example, the 'anterior spiracle' is an instance of its parent term 'spiracle'. The second is 'part of'; for example, the 'gastric caecum' is part of the 'foregut'. The third is 'develops from'; for example, a 'glial cell' develops from a 'glioblast'.

The major change that had to be made to the FlyBase controlled vocabulary to support this project was to name the developmental intermediates that arise during embryogenesis, that is anlagen, primordia, and anlagen in statu nascendi. Our annotation uses a subset of 300 or so of the 5,800 terms in the FlyBase controlled vocabulary, many of which only apply to later stages of development.

We modified the GO database schema [25] for the storage and searching of our gene-expression data. For the management of the terms and their relationships, the core of the GO database schema remains essentially unchanged. However, the database was extended to support the annotation process itself; that is, assigning terms to describe the expression patterns. Additional tables were also added to describe when and where a given mRNA is expressed, and the images that constitute the evidence for these observations.

We implemented two publicly available tools to search and mine the gene-expression dataset. The advanced search page is a modified version of the Gadfly search interface [26,27]. It can be utilized to search for the expression pattern of an individual gene of interest, retrieve a list of genes expressed in a given embryonic structure, or set of structures, or all genes expressed at a certain stage of embryonic development. Sets of genes and their corresponding expression profiles can be grouped on the basis of cytological position in the genome, functional GO assignments, or the presence of protein domains in the gene sequence. The results returned by all types of searches can be formatted to display controlled vocabulary annotations exclusively or also show images and microarray profiles of sets of genes side by side (Figure 7). Alternatively, one can explore the dataset by browsing through the controlled vocabulary using a modified version of the Amigo Gene Ontology browser, which we call ImaGO [28]. Once a term from the vocabulary is selected, ImaGO will return a page that lists all genes expressed in a given structure and also all genes expressed in all structures that descend from it.

### Systematic analysis of the *in situ* data

The embryonic expression patterns of 80% of the 1,388 genes that display restricted expression, and were therefore

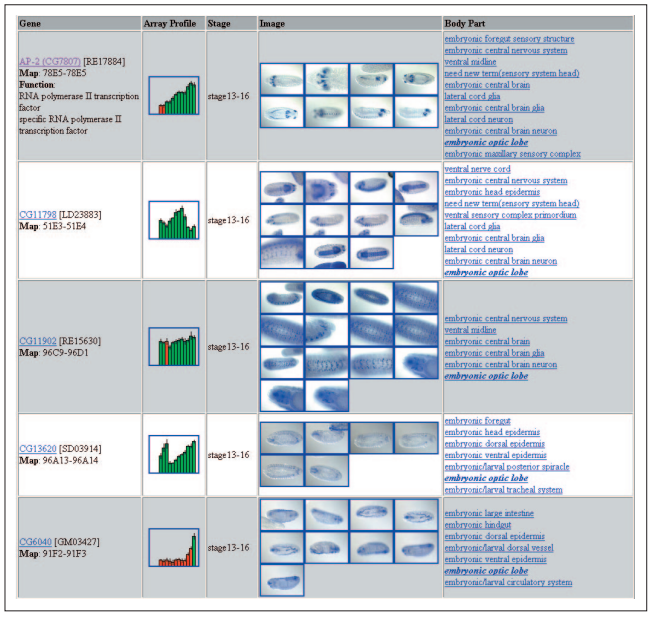


**Figure 7**
Screenshot of the result page of our publicly available search tool. The first four of the 14 genes returned by a query for genes expressed in the 'embryonic optic lobe' are shown. The 'Gene' column gives the gene name, gene identifier, EST identifier, cytological position and GO function assignments, where available. The gene name serves as a link to access the complete expression report page for that gene. Array profiles and images can be enlarged in a separate window by clicking on the thumbnail image. In the column labeled 'Body Part' is a list of all annotation terms that have been assigned to that gene, with the query subject (in this case, embryonic optic lobe) highlighted by bold italics. Each annotation term is hyperlinked to the ImaGO Gene Ontology browser.

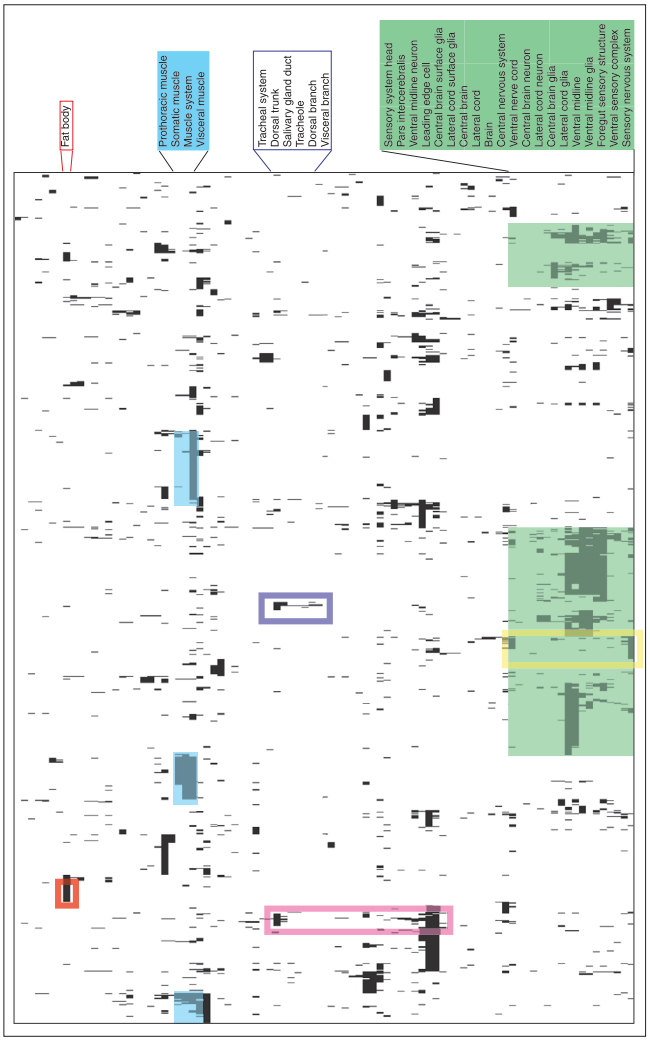


**Figure 8**
Hierarchical clustering of controlled vocabulary annotations. Columns of the matrix represent the 99 annotation terms from the controlled vocabulary that correspond to differentiated organs. Rows of the matrix represent 1,257 genes that are expressed in at least one of those embryonic structures. A black matrix cell indicates that a gene is expressed in the given structure. Both rows and columns are clustered using a binary distance metric and hierarchical complete linkage clustering. Green shading highlights clusters of embryonic structures that are part of the nervous system, cyan shading highlights clusters formed by components of the muscle system. Genes expressed specifically in the embryonic fat body are highlighted by a red rectangle, two separate clusters of genes expressed in the tracheal system are surrounded by blue and magenta rectangles. A cluster of genes expressed in the peripheral nervous system and not in the central nervous system is enclosed by the yellow rectangle.

annotated in our database, are described by a unique set of annotation terms. This observation illustrates the tremendous diversity of gene-expression patterns during embryogenesis, which range from expression in a single embryonic structure to expression in 36 distinct tissues. Although expression patterns of genes are rarely identical, there is a noticeable similarity among patterns of expression of many genes. Therefore we sought to order these genes on the basis of the similarity of their expression patterns. Furthermore, gene-expression data can be used to quantify the relatedness of the various embryonic structures in terms of similarity in gene expression between them [29]. We carried out hierarchical clustering of genes and tissues using a method based on binary similarity metrics ([30]; for details see Materials and methods). Figure 8 shows the result of clustering the 99 differentiated embryonic structures that expressed at least two of the 1,388 genes. A black dash at the intersection of a row and a column of the matrix occurs whenever the gene corresponding to that row is expressed in the embryonic structure corresponding to that column.

The clustering organizes the embryonic structures in such a way that related structures are close together whereas unrelated ones are widely separated. For example, components of the nervous system (Figure 8, green shading) that are ectoderm derivatives, cluster together and away from mesodermal derivatives, such as muscles (Figure 8, cyan shading). In other words, very few of the genes in our dataset are expressed in both muscles and the nervous system,

reflecting the physiological separation and different developmental origins of these two tissues.

By analogy, the genes are organized by the hierarchical clustering so that those with the most similar expression patterns are close together and those with highly divergent patterns are widely separated. The distribution of clusters in the matrix can be used to identify genes that are expressed in a tissue or set of tissues. For example, the red rectangle in Figure 8 highlights a cluster of genes that are expressed exclusively in the embryonic fat body. Genes expressed in the tracheal system are split into at least two clusters; genes expressed exclusively in the trachea form a cluster in the middle of the matrix (Figure 8, blue rectangle), and a second cluster includes genes expressed in the trachea and variety of epidermal structures (Figure 8, magenta rectangle). Interestingly, no genes are expressed in both trachea and the CNS (note the gap in CNS clusters at the level of the tracheal cluster). Genes expressed in the nervous system form the most prominent clusters. The annotation vocabulary subdivides the nervous system into specific subsets based on tissue types (neurons, glia) and anatomical position (brain, ventral nerve cord, lateral cord, sensory nervous system). A cluster of genes that are expressed specifically in the components of the peripheral nervous system and absent from CNS can be identified (Figure 8, yellow rectangle). An increase in the depth of annotation will be required to subdivide the large clusters that correspond to complex organ systems.

Figure 8 represents one possible outcome of the clustering analysis of the annotation dataset. Filtering of the genes and anatomical structures, the type of clustering algorithm and the distance metric are variables that need to be optimized to address specific questions about the variations in patterns of gene expression. We used a relatively simple metric to define similarity among the annotation data. In the future it will be interesting to explore more complex similarity metrics that incorporate the distance between annotation terms within the ontology. Clustering of the annotation data and other data-mining approaches will establish sets of co-regulated genes that will provide a starting point for investigating *cis*-regulatory sequences that may elucidate novel regulatory relationships in development. Interactive web pages with a complete clustering matrix can be accessed at [31].

Systematic RNA *in situ* hybridization is an alternative to mutagenesis screens [32] to uncover genes involved in embryonic patterning. Figure 9a-d illustrates one case where conventional mutagenesis failed to identify genes with highly specific expression patterns at the cellular blastoderm stage, most probably because of genetic redundancy. At map position 66E4, three adjacent and highly homologous genes for Brachyury/T-box-containing transcription factors are expressed with strikingly similar expression patterns. Thus disruption of any one of these genes might not be sufficient to produce an embryonic phenotype. Conversely, in many cases the expression patterns of duplicated genes have diverged and are largely non-overlapping. Expression data can provide a guide as to which multiple gene knockouts are likely to yield specific phenotypes.

A systematic screening approach also reduces bias in the selection of the types of genes chosen for study. Figure 9e-i shows five examples of metabolic genes that, contrary to naive expectation, are expressed at cellular blastoderm in domains suggestive of roles in embryonic patterning. A similar observation was recently reported for the expression of genes isolated specifically from blastoderm-specific cDNA libraries [7]. Tight regulation of expression of these genes could be explained by a preferential requirement for certain metabolic pathways in specialized embryonic tissues. That argument may not be plausible for genes expressed within limited regions of the cellular blastoderm embryo. It is possible that these gene products are not translated, are otherwise inactive in the tissues where the transcripts appear abundant, or that their restricted expression is simply the result of their proximity to a transcriptional control element of a neighboring gene. A more interesting possibility is that this expression may reflect yet unknown functions of these genes.

A major advantage of RNA *in situ* hybridization is that this method has sufficient spatial resolution to uncover subcellular localization of mRNAs. Figure 9j,l shows an apically localized mRNA in the columnar epithelium of the developing hindgut surrounding the migrating pole cells (Figure 9l). This staining is strikingly complementary to that of a basally localized mRNA from a different gene that is expressed in the same cells (Figure 9k,m). The transcript of yet another gene, whose expression is shown at high magnification at the pre-cellular blastoderm stage, appears to be localized to a sub-compartment of the nucleus (Figure 9n,o). We also found novel mRNAs localized asymmetrically along the anterior-posterior axis of the early pre-blastoderm embryo (data not shown). Overall, we find that about 1% of genes exhibit easily discernible subcellular localization, and thus our dataset can also be useful in identifying aspects of RNA localization and trafficking.

## Conclusions

The dataset we present here comprises embryonic expression patterns for about one-sixth of all *Drosophila* genes, documented with extensive digital images, controlled vocabulary annotations and microarray profiles. Our ultimate goal is to determine the expression patterns of all genes in the genome. Considering our current production rate, we should be able to finish the first pass through the existing cDNA collections that represent about 70% of all *Drosophila* genes in about a year. We will then repeat our analysis of the 20% or so of genes for which we did not obtain reliable data. Probes for genes that lack a suitable cDNA clone, but that show significant expression by microarray analysis, will be generated by genomic PCR

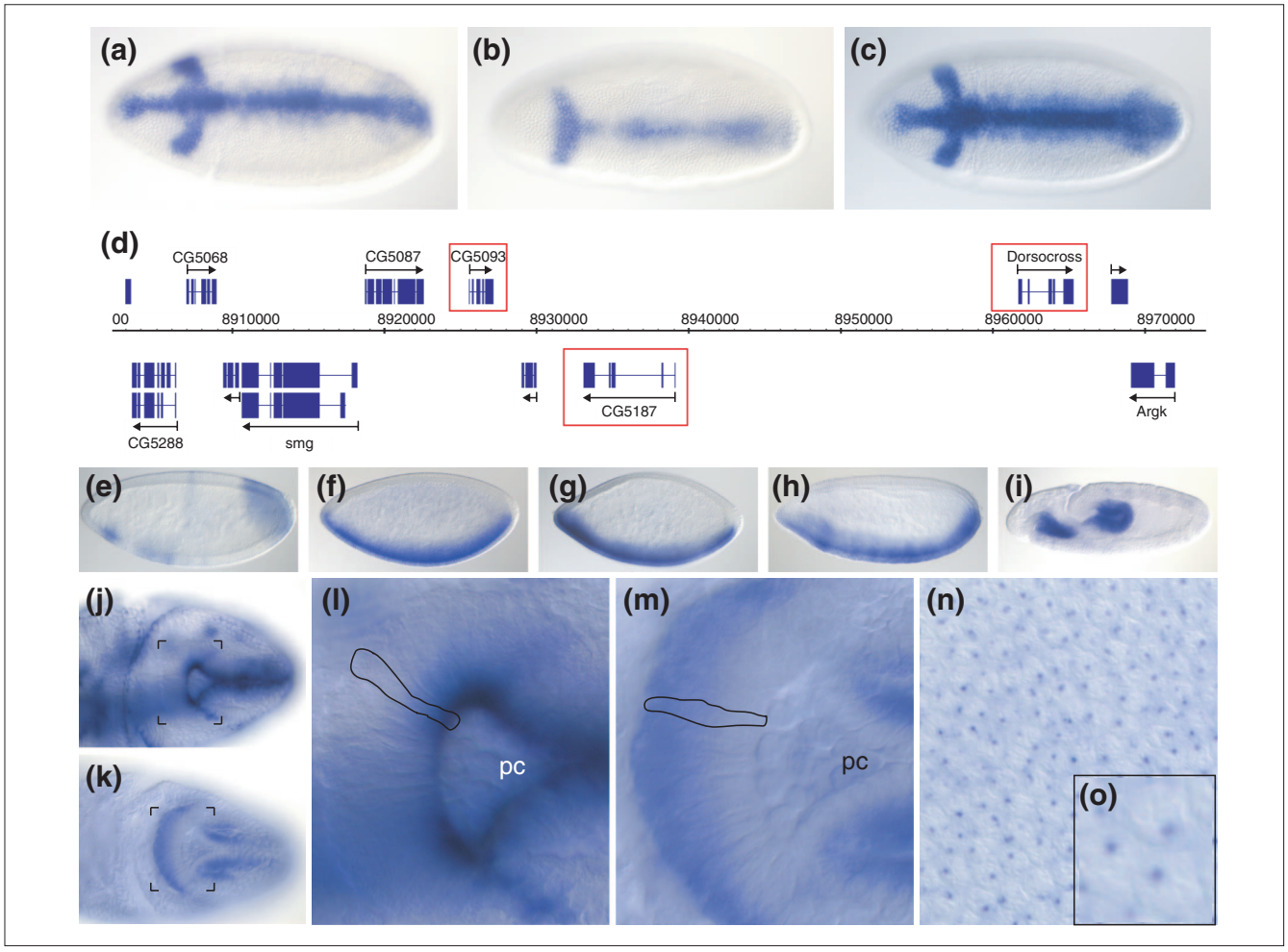


**Figure 9**
Examples of interesting observations from this project. **(a-d)** Three adjacent Brachyury/T-box genes - (a) *CG5093*, (b) *CG5107*, (c) *Dorsocross* - show remarkably similar expression patterns at cellular blastoderm and are located next to each other on the chromosome (d). **(e-i)** Expression patterns of five genes with homology to metabolic and detoxification enzymes: (e) hydroxyacylglutathione hydrolase, *CG9026*; (f), cytochrome P450, *Cyp310a;* (g) multi-drug resistance gene, *Mdr49*; (h) xanthine dehydrogenase, *rosy*; and (i) transketolase, *CG8036*. **(j)** Dorsal view of a stage-8 embryo stained with a probe that reveals apically localized mRNAs (*CG18375*) within the developing hindgut epithelium, contrasted with basally localized mRNA (*CG11207*) in the same cells **(k)**. **(l)** Close-up of (j) highlighting the apically localized mRNA in the epithelium surrounding the invaginating hindgut pocket with pole cells (pc). A single epithelial cell is outlined. **(m)** Close-up of (K) revealing an equivalent region of an embryo as (l) and highlighting the basally localized mRNA. **(n)** Portion of the dorsal side of a pre-blastoderm embryo stained for mRNA (*CG1962*) that appears to be localized to an unidentified subnuclear compartment. **(o)** Close-up of five nuclei from (n).

so that eventually all *Drosophila* genes will be examined. We also intend to extend our analysis to two other developmentally active *Drosophila* tissues - imaginal discs and ovaries.

All our data are freely available to the scientific community through interactive web pages; these pages will continue to develop and will allow for more sophisticated mining of the growing dataset. Similar large-scale gene-expression studies have been carried out in other model organisms including *Xenopus* [33], mouse [34], medaka [35] and *Caenorhabditis elegans* [36]. Our database is, to our knowledge, the first to use non-redundant expressed sequence tag (EST) collections with the aim of determining and systematically annotating the expression patterns of all genes in an organism. We intend to link our database to the available public databases containing similar image data in order to allow cross-species comparisons of expression of homologous genes. The ultimate goal is to create an integrated resource of image oriented gene-expression data analogous to the public repositories of DNA sequences.

## Materials and methods

### 96-well *in situ* hybridization

Canton S embryos were collected in 3-h intervals and aged to generate animals 0-3, 3-6, 6-9, 9-12, 12-15 and 15-18 h old.

The embryos were then dechorionated, devitelinized, and stored in methanol at -20°C. The six 3-h embryo collections were mixed in equal proportions to yield a balanced population of embryos representing the first 18 h of embryogenesis.

DNA templates were generated by PCR using primers homologous to the vector and purified by G50 column chromatography in 96-well format. The purified PCR product (5 μl) was transcribed in 96-well format by incubation for 2 h at 37°C after the addition of 5 μl of a polymerase reaction cocktail consisting of 2 U T7 RNA polymerase, 4.6 U RNase inhibitor, 10 mM NTPs, 3.5 mM digoxigenin-11-UTP, 40 mM Tris pH 8.0, 6 mM $MgCl_2$, 10 mM DTT and 2 mM spermidine. After treatment with DNase I and $Na_2CO_3$ pH 10.2, ethanol precipitation was carried out. Pellets were resuspended in 50 μl of 50% formamide, 5 mM Tris-HCl pH 7.5, 0.5 mM EDTA and 0.01% Tween 20.

The digoxigenin-labeled RNA probe was quantified by immunological detection using a modified digoxigenin quantification protocol (Roche). A sample of 0.8 μl of a 1:300 dilution of the probe was spotted on a positively charged nylon membrane (Roche) with a 96-well pin tool (V&P Scientific) and then cross-linked to the membrane by UV irradiation. The membranes were then treated with anti-digoxigenin-AP Fab fragments and the color substrates NBT/BCIP. The quality of each probe was determined by comparing the intensity of individual probe spots to spots containing 3, 10, 30, 100 or 300 pg of control probes.

Re-hydrated and post-fixed embryos were incubated for 1 h in hybridization buffer (50% formamide, 4x SSC, and 0.01% Tween 20). Twenty microliters of these embryos were gently placed in each well of a 96-well filter plate (Millipore MADV N65) with a multi-channel pipette (Brand Transferpette-12) using wide-orifice 250 μl pre-sterilized tips (Rainin). Digoxigenin-labeled RNA probe (200 μl of a 1:100 dilution in hybridization buffer with 5% dextran sulfate) was added and the embryos were incubated overnight at 55°C. Gentle vacuum was used to remove the hybridization solution and the embryos were subjected to eight 30-min washes in wash buffer (50% formamide, 2x SSC and 0.01% Tween 20). The embryos were treated for 2 h with 5% goat serum (Roche) and anti-digoxigenin-AP Fab fragments (Roche). Following nine 10-min washes in 0.1% Tween 20 in PBS and two rinses in AP buffer (50 mM $MgCl_2$, 100 mM NaCl, 100 mM Tris pH 9.5, 0.01% Tween 20) the NBT/BCIP color substrates were used to detect the hybridized probes. Embryos were washed six times with ethanol to enhance contrast and stored in 70% glycerol in PBS. The quality of the hybridization signal, the morphology of the embryos and the number of patterns were assessed under a low-power microscope.

### Digital imaging

Low-magnification images were taken using a dissecting microscope (Leica Wild M10) equipped with a ProgRes 3012 digital camera. Usually two images at different magnifications were captured. High-resolution images were captured with a Spot RT digital camera mounted onto a Zeiss Axiophot equipped with Nomarski optics. The majority of images were taken with either a 20x or 40x objective. All images were saved as JPEG files.

Often several focal planes of the same embryo were captured to fully document the spatial distribution of the staining pattern. In many cases embryos were manually repositioned to provide a more favorable angle for documenting the expression pattern. When a whole embryo view was insufficient to visualize the fine aspects of the staining pattern, we captured a higher-magnification image focused on a small part of the embryo. Such higher-resolution images were generally accompanied by corresponding lower-magnification images for orientation purposes. Most images show the embryo with anterior to the left and dorsal side up; however, the orientation of images captured in the early stages of the project do not consistently follow this rule.

### Microarray analysis

Canton S flies were seeded into 12 population cages and aged in the collection cages for three days with fresh food provided every 12 h. In the morning of the fourth day, the flies were allowed to pre-lay retained embryos. Fresh plates were then introduced simultaneously into all 12 cages and embryos were collected for 1 h. The embryos were then transferred into a 25°C incubator and aged. At appropriate time points, embryos were dechorionated and quick-frozen in liquid nitrogen. This procedure yielded 12 samples of non-overlapping 1-h collections starting from 30 to 90 min and ending at 11.5 h to 12.5 h post egg laying. This procedure was carried out for 3 days, yielding three replicates of each time window. A sampling of each collection was set aside, devitelinized, and stored in methanol at -20°C. These embryos were used to determine the distribution of stages in each collection sample by examination of morphological markers. These data were then used to construct an approximate time line correlating the embryo collections and embryonic stages (see Figure 4).

Total RNA was isolated from the 12 embryo samples described above by homogenization with a motorized plastic pellet pestle in Ambion RNAwiz solution, followed by chloroform extraction and ethanol precipitation. Eight micrograms of total RNA were used to generate digoxigenin-labeled fragmented cRNA using a standard Affymetrix amplification and labeling protocol. cRNA was hybridized to a GeneChip *Drosophila* Genome Array using standard Affymetrix equipment and protocols. The scanned array images were analyzed using Affymetrix Microarray Suite and dChip software [37]. We collected 36 GeneChip array scans and the success of the experiments was determined by the reproducibility of the three independent replicates. Two of the 36 experiments were

repeated to gain higher-quality data. Microarray data are being submitted to Array Express as E-RUBN-2.

Signals from all replicate experiments were averaged and the standard error of the three measurements was calculated. Data were entered into a custom-designed MySQL database and graphs of the microarray time-course for all 14,000 genes were generated using custom Perl scripts and a GD graphics library. The absent/present calls generated by Affymetrix Microarray Suite were color-coded (present = green, absent = red, marginal = blue) and incorporated into graphs based on dChip-derived data. The array-based expression profiles were incorporated into the annotation, report, and analysis web pages described below.

### Image data annotation and presentation

We built a multi-platform network consisting of two Microsoft Windows workstations connected to digital cameras on microscope equipment and a Suse Linux server running an Apache HTTP server and MySQL database. Image data and annotations were submitted to the production MySQL database through a Perl-based annotation tool (Figure 2). The annotation tool displays microarray data linked to the cDNA under investigation as well as a compilation of available information about that gene in the form of external database links, protein domains and GO terms (from FlyBase [38]). The annotation tool permits the entering of production-level assessments about the quality and identity of the captured images. Several other web-based tools were developed that support the entering of additional data (Figure 1a-d) as well as report scripts that summarize the captured data.

Periodically, the data from the production database were transferred into a second MySQL database that uses a schema modified from that of the GO database. In conjunction with the Gadfly database and Application Programming Interface (see [27]), this database allows gene-based and anatomy-based searches of the dataset [26].

The controlled vocabulary used to annotate the gene-expression profiles is a subset of the FlyBase controlled vocabulary for anatomy and development [39]. Most annotation terms can be found under the 'developing embryonic structure' branch of this ontology. We developed a modified version of the Amigo Gene Ontology Browser, ImaGO [28], which incorporates the anatomy ontologies and the image data. ImaGO can be used to browse through and search the data by anatomical structures. A more concise version of the annotation hierarchy containing only the terms found in the annotation tool can be accessed at [40].

### Clustering of annotation data

Annotation data were converted into a binary matrix, the rows representing the genes and the columns representing the anatomical structures. When a given gene was expressed in a given anatomical structure the intersection in the matrix was 1; otherwise it was 0. The matrix was loaded into an R statistics package and dissimilarity matrices were calculated for each two rows and each two columns of the dataset. The distance measure was (b + c)/(a + b + c), where a is the frequency of 11 columns in two rows of binary data, b is the frequency of 10 columns and c is the frequency of 01 columns. Using the dissimilarity matrices, anatomical structures and genes were clustered sequentially using hierarchical clustering with a complete linkage agglomeration method. Clustered matrices were exported from R and converted into interactive web pages using a custom Perl script. The binary data were color-coded; black indicates that the gene is on in a structure, white indicates that expression of the gene is not detected in that structure.

## Acknowledgements

We thank Audrey Huang for helpful comments on the manuscript, Terry Speed (University of California, Berkeley) for valuable advice on clustering of binary data, Bradley Marshall for modification of the AmiGO interface and Ben Berman for useful discussions. Trina Agbayani and Joseph Nunoo provided technical assistance in the early stages of this project. This work was supported by the Howard Hughes Medical Institute and by NIH Grants P50 HG00750 (to G.R.) and P41 HG00739 (to W. Gelbart).

## References

1. Pollet N, Niehrs C: **Expression profiling by systematic high-throughput *in situ* hybridization to whole-mount embryos.** *Methods Mol Biol* 2001, **175:**309-321.
2. Lipshutz RJ, Fodor SP, Gingeras TR, Lockhart DJ: **High density synthetic oligonucleotide arrays.** *Nat Genet* 1999, **21(Suppl)**:20-24.
3. Lockhart DJ, Dong H, Byrne MC, Follettie MT, Gallo MV, Chee MS, Mittmann M, Wang C, Kobayashi M, Horton H, *et al.*: **Expression monitoring by hybridization to high-density oligonucleotide arrays.** *Nat Biotechnol* 1996, **14:**1675-1680.
4. Brown PO and Botstein D: **Exploring the new world of the genome with DNA microarrays.** *Nat Genet* 1999, **21(Suppl):**33-37.
5. Jones KW, Robertson FW: **Localisation of reiterated nucleotide sequences in *Drosophila* and mouse by *in situ* hybridisation of complementary RNA.** *Chromosoma* 1970, **31:**331-345.
6. Harrison PR, Conkie D, Paul J, Jones K: **Localisation of cellular globin messenger RNA by *in situ* hybridisation to complementary DNA.** *FEBS Lett* 1973, **32:**109-112.
7. Simin K, Scuderi A, Reamey J, Dunn D, Weiss R, Metherall JE, Letsou A: **Profiling patterned transcripts in *Drosophila* embryos.** *Genome Res* 2002, **12:**1040-1047.
8. Kopczynski CC, Noordermeer JN, Serano TL, Chen WY, Pendleton JD, Lewis S, Goodman CS, Rubin GM: **A high throughput screen to identify secreted and transmembrane proteins involved in *Drosophila* embryogenesis.** *Proc Natl Acad Sci USA* 1998, **95:**9973-9978.
9. Furlong EE, Andersen EC, Null B, White KP, Scott MP: **Patterns of gene expression during *Drosophila* mesoderm development.** *Science* 2001, **293:**1629-1633.
10. Kim SK, Lund J, Kiraly M, Duke K, Jiang M, Stuart JM, Eizinger A, Wylie BN, Davidson GS: **A gene expression map for *Caenorhabditis elegans*.** *Science* 2001, **293:**2087-2092.
11. Spellman PT, Sherlock G, Zhang MQ, Iyer VR, Anders K, Eisen MB, Brown PO, Botstein D, Futcher B: **Comprehensive identification of cell cycle-regulated genes of the yeast *Saccharomyces cerevisiae* by microarray hybridization.** *Mol Biol Cell* 1998, **9:**3273-3297.
12. Chudin E, Walker R, Kosaka A, Wu SX, Rabert D, Chang TK, Kreder DE: **Assessment of the relationship between signal**

**intensities and transcript concentration for Affymetrix GeneChip arrays.** *Genome Biol* 2001, **3**:research0005.1-0005.10
13. Schena M, Shalon D, Davis RW, Brown PO: **Quantitative monitoring of gene expression patterns with a complementary DNA microarray.** *Science* 1995, **270:**467-470.
14. Rubin GM, Hong L, Brokstein P, Evans-Holm M, Frise E, Stapleton M, Harvey DA: **A *Drosophila* complementary DNA resource.** *Science* 2000, **287:**2222-2224.
15. Stapleton M, Liao G, Brokstein P, Hong L, Carninci P, Shiraki T, Hayashizaki Y, Champe M, Pacleb J, Wan K, *et al.*: **The *Drosophila* gene collection: identification of putative full-length cDNAs for 70% of *D. melanogaster* genes.** *Genome Res* 2002, **12:**1294-1300.
16. Stapleton M, Carlson J, Brokstein P, Yu C, Champe M, George R, Guarin H, Pacleb J, Park S, Wan K, *et al.*: **A *Drosophila* full-length cDNA resource.** *Genome Biol* 2002, **3**:research0080.1-0080.8
17. Hartenstein V, Campos-Ortega JA: *The Embryonic Development of* Drosophila melanogaster, 2nd edn. Heidelberg: Springer-Verlag; 1997.
18. **Patterns of gene expression in *Drosophila* embryogenesis** [http://www.fruitfly.org/cgi-bin/ex/insitu.pl]
19. Tautz D, Pfeifle C: **A non-radioactive *in situ* hybridization method for the localization of specific RNAs in *Drosophila* embryos reveals translational control of the segmentation gene hunchback.** *Chromosoma* 1989, **98:**81-85.
20. Bownes M: **A photographic study of development in the living embryo of *Drosophila melanogaster*.** *J Embryol Exp Morphol* 1975, **33:**789-801.
21. Arbeitman MN, Furlong EE, Imam F, Johnson E, Null BH, Baker BS, Krasnow MA, Scott MP, Davis RW, White KP: **Gene expression during the life cycle of *Drosophila melanogaster*.** *Science* 2002, **297:**2270-2275.
22. Crews ST, Thomas JB, Goodman CS: **The *Drosophila single-minded* gene encodes a nuclear protein with sequence similarity to the *per* gene product.** *Cell* 1988, **52:**143-151.
23. The FlyBase Consortium: **The FlyBase database of the *Drosophila* genome projects and community literature.** *Nucleic Acids Res* 2002, **30:**106-108.
24. Ashburner M, Ball CA, Blake JA, Botstein D, Butler H, Cherry JM, Davis AP, Dolinski K, Dwight SS, Eppig JT, *et al.*: **Gene ontology: tool for the unification of biology. The Gene Ontology Consortium.** *Nat Genet* 2000, **25:**25-29.
25. **Gene Ontology database - GO database schema** [http://www.godatabase.org/dev/database]
26. **BDGP gene expression query interface** [http://www.fruitfly.org/cgi-bin/ex/basic.pl]
27. Mungall CJ, Misra S, Berman BP, Carlson J, Frise E, Harris N, Marshall B, Shu S, Kaminker JS, Prochnik SE, *et al.*: **An integrated computational pipeline and database to support whole genome sequence annotation.** *Genome Biol* 2002, **3:**research0081.1-0081.11
28. **ImaGO** [http://www.fruitfly.org/cgi-bin/ex/go.cgi]
29. Pollet N, Schmidt HA, Gawantka V, Niehrs C, Vingron M: ***In silico* analysis of gene expression patterns during early development of *Xenopus laevis*.** *Pac Symp Biocomput* 2000:443-454.
30. Eisen MB, Spellman PT, Brown PO, Botstein D: **Cluster analysis and display of genome-wide expression patterns.** *Proc Natl Acad Sci USA* 1998, **95:**14863-14868.
31. **Annotation clustering** [http://www.fruitfly.org/ex/annotation_clustering.html]
32. Nusslein-Volhard C, Wieschaus E: **Mutations affecting segment number and polarity in *Drosophila*.** *Nature* 1980, **287:**795-801.
33. Gawantka V, Pollet N, Delius H, Vingron M, Pfister R, Nitsch R, Blumenstock C, Niehrs C: **Gene expression screening in *Xenopus* identifies molecular pathways, predicts gene function and provides a global view of embryonic patterning.** *Mech Dev* 1998, **77:**95-141.
34. Neidhardt L, Gasca S, Wertz K, Obermayr F, Worpenberg S, Lehrach H, Herrmann BG: **Large-scale screen for genes controlling mammalian embryogenesis, using high-throughput gene expression analysis in mouse embryos.** *Mech Dev* 2000, **98:**77-94.
35. Henrich T, Wittbrodt J: **An *in situ* hybridization screen for the rapid isolation of differentially expressed genes.** *Dev Genes Evol* 2000, **210:**28-33.
36. **NEXTDB: the nematode expression pattern database** [http://nematode.lab.nig.ac.jp/index.html]
37. Li C, Hung Wong W: **Model-based analysis of oligonucleotide arrays: model validation, design issues and standard error application.** *Genome Biol* 2001, **2**:research0032.1-0032.11.
38. **FlyBase** [http:www.flybase.org]
39. **FlyBase controlled vocabulary for anatomy** [http://flybase.bio.indiana.edu/docs/lk/bodyparts-cv.txt]
40. **Annotation hierarchy** [http://www.fruitfly.org/cgi-bin/ex/insitu_hierarchy.pl]